

# Interference between magnetic field and cavity modes in an extended Josephson junction

V. Humbert,<sup>1</sup> M. Aprili,<sup>1,\*</sup> and J. Hammer<sup>2,†</sup>

<sup>1</sup>Laboratoire de Physique des Solides, UMR8502-CNRS, University Paris-Sud, 91405 Orsay Cedex, France

<sup>2</sup>Institute for Experimental and Applied Physics, University of Regensburg, 93040 Regensburg, Germany

(Received 14 December 2011; revised manuscript received 27 April 2012; published 20 July 2012)

An extended Josephson junction consists of two superconducting electrodes separated by an insulator and is therefore also a microwave cavity. The superconducting phase difference across the junction determines the amplitude as well as the spatial distribution of the supercurrent. Both external magnetic fields and resonant intracavity fields produce a spatial modification of the superconducting phase along the junction. The interplay between these two effects leads to interference in the critical current of the junction and allows us to continuously tune the coupling strength between the first cavity mode and the Josephson phase from 1 to  $-0.68$ . This enables static and dynamic control of the junction in the ultrastrong-coupling regime.

DOI: [10.1103/PhysRevB.86.024520](https://doi.org/10.1103/PhysRevB.86.024520)

PACS number(s): 74.81.Fa, 74.50.+r, 74.78.Na, 42.87.Bg

## I. INTRODUCTION

A Josephson junction can be described as a two level system, at sufficiently low temperature, due to the nonlinearity of the Josephson coupling. The strong coupling of a Josephson junction to an on-chip microwave superconducting resonator with small losses (i.e., quality factor higher than  $10^4$ ) has led to the emergence of the field of circuit quantum electrodynamics (CQED).<sup>1</sup> We note that an extended Josephson junction in which the two superconductors are coupled through an insulating barrier is at the same time a nonlinear Josephson oscillator *and* a microwave cavity.<sup>2</sup> Neglecting the Josephson effect, the eigenfrequencies of the electromagnetic modes are given by  $\nu_n = k_n \cdot c_s / 2\pi$ , with  $k_n = n \cdot \pi / L$  where  $L$  is the junction length [see Fig. 1(b)] and  $c_s$  the Swihart velocity.<sup>3</sup> As the Josephson current and the microwave field are both localized in the insulator, extended junctions intrinsically form a microwave cavity enclosing a material resonance, the superconducting oscillator. At low temperature the Josephson plasma frequency and the mode frequencies can therefore be made much larger than damping, as required for strong coupling. Even more importantly this system allows tuning of the vacuum Rabi frequency, i.e., the photon exchange rate between the microwave cavity and the Josephson oscillator, to be as large as a fraction of the first cavity mode eigenfrequency. The latter requirement shows that the system is in fact in the ultrastrong-coupling limit.<sup>4</sup> This can be seen from the Hamiltonian of the junction,<sup>5</sup>  $H = H_J + H_c + H_{\text{int}}$  where  $H_J$  and  $H_c$  are the Josephson and the cavity Hamiltonian, respectively, while  $H_{\text{int}} = -(h\nu_p)^2 / h\nu_n g_n N_c \varphi_0$  describes the interaction between the cavity modes and the Josephson phase. Here  $\nu_p$  is the Josephson plasma frequency,  $N_c$  is the cavity photon number, and  $\varphi_0$  is the macroscopic phase difference across the junction.<sup>6</sup> The interaction thus provides an intrinsically nonlinear coupling which is formally equivalent to radiation-pressure interaction in optomechanics.<sup>7,8</sup> The coupling constant  $g_n$  is given by

$$g_n = 2 \int_{-L/2}^{L/2} \frac{dx}{L} \sin[k_n x]^2 \cos[k_H x] = \frac{\sin\left[\frac{\pi\phi}{\phi_0}\right]}{\frac{\pi\phi}{\phi_0}} \cdot h_n(\phi) \quad (1)$$

$$\text{with } h_n(\phi) = 1 + \frac{(\phi/\phi_0)^2 \cos(n\pi)}{n^2 - (\phi/\phi_0)^2},$$

where  $k_H = 2\pi\phi/(\phi_0 L)$ , with  $\phi$  the magnetic flux in the junction and  $\phi_0 = 2e/h$  the flux quantum.<sup>5</sup> At zero applied magnetic field  $g_1 = 1$ , therefore extended Josephson junctions provide an appealing system to investigate ultrastrong coupling between the superconducting phase and photons<sup>9</sup> with little perturbations from the electromagnetic environment. This regime is difficult to achieve in optical cavities,<sup>10</sup> but recently has been obtained in a solid-state semiconductor system.<sup>11</sup> Furthermore it is worth noting that the coupling is statically and dynamically tunable. In fact,  $g_1$  can be continuously changed from 1 to  $-0.68$  by the external magnetic field.

In this paper we report on the magnetic field dependence of the coupling strength between the Josephson phase and the first cavity mode. Here  $g_1$  is obtained by measuring the Josephson critical current as a function of the applied magnetic field for a microwave radiation frequency either resonant or nonresonant with the first cavity mode. Thus the magnetic field dependence of  $g_1$  corresponds physically to the interference in the Josephson critical current between the phase differences produced by the intracavity and the magnetic fields.

The critical current of a planar rectangular Josephson junction shows a Fraunhofer pattern as a function of the applied magnetic field<sup>12</sup> [see Fig. 1(c)]. This originates from the phase difference  $\varphi_H$ , created by the magnetic flux through the junction.<sup>13</sup> If self-screening of the applied magnetic field is neglected (i.e.,  $\lambda_L \gg L$  where  $\lambda_L$  is the Josephson penetration depth), the phase difference accumulated along the junction is  $\varphi_H = k_H x$ . Therefore the critical current  $I_c$  through the junction is given by  $I_c = I_{c0} \left| \frac{\sin(\pi\phi/\phi_0)}{\pi\phi/\phi_0} \right|$ .<sup>13</sup>

In presence of a microwave resonant field due to microwave excitation, the phase difference produced by the electromagnetic field,  $\varphi_{RF}$ , has to be added to  $\varphi_H$ . The total phase difference is  $\varphi = \varphi_H + \varphi_{RF} + \varphi_0$  where  $\varphi_{RF} = a_n \cdot \text{Re}(e^{i2\pi\nu_n t}) \sin(k_n x)$  is obtained by integrating the second Josephson equation with  $a_n = 2eV_{RF}/(\hbar\nu_n)$ . The critical current through the junction after integration of the first Josephson equation over time and space becomes<sup>5</sup>

$$I_c = I_{c0} \left| \frac{\sin(\pi\phi/\phi_0)}{\pi\phi/\phi_0} \right| \cdot \left( 1 - \frac{a_n^2}{4} \cdot h_n(\phi) \right). \quad (2)$$

Therefore the intracavity field of each mode contributes differently to the diffraction pattern. The second term in

Eq. (2) gives the magnetic field dependence of the coupling strength to the  $n$ th resonant mode,  $g_n$ , and it accounts for the interference in the critical current originating from  $\varphi_H$  and  $\varphi_{RF}$ . For simplicity we consider only the first mode, resulting in a magnetic field dependent deviation of the critical current according to

$$\Delta I_c = I_{c0} \frac{a_1^2}{4} g_1(\phi) \cdot \text{sgn}\left(\frac{\sin(\pi\phi/\phi_0)}{\pi\phi/\phi_0}\right). \quad (3)$$

Consequently by measuring the change in the critical current as a function of the magnetic flux, we obtain the coupling constant  $g_1$ . It is important to point out that in the experiment presented below, we only address the coupling constant, while the superconducting phase and the electromagnetic field are classical fields and the number of microwave photons in the cavity (ranging from  $10^4$  to  $10^5$ ) is far from that needed for a single-photon experiment. This is simply due to the junction parameters and particularly to the junction area, however the value of the coupling constant  $g_1$  does not change in the quantum limit. Thus it is in principle possible and quite simple to change the junction geometry to get into the ultrastrong-coupling quantum regime.

Let us make a few remarks about Eq. (3). First, since the phase-intrafield coupling is not linear,  $\Delta I_c$  as a function of the magnetic flux is not equivalent to a normalization of the critical current and/or of magnetic quantum flux in the junction. Second  $\Delta I_c$  changes sign at  $0.7\phi_0$ , meaning that the overall effect of microwave radiation is to decrease the critical current through the junction for  $\phi < 0.7\phi_0$ , while it is to increase  $I_c$  for  $\phi > 0.7\phi_0$ . This is contrary to the common belief that microwave fields always reduce the Josephson critical current in the adiabatic approximation, i.e., when phase-photon coupled dynamics is not taken into account.<sup>14</sup> Finally from the Josephson current-phase relation  $I = I_c \sin(\varphi)$  we observe that there is a small flux range just above  $\phi_0$  in which the macroscopic phase difference through the junction changes from  $\pi$  to 0 under resonant microwave irradiation at frequency  $\nu_1$ . This is because close to  $\phi_0$ , the effect of the interference term  $\Delta I_c$  is equivalent to a small shift in the Fraunhofer pattern. In long superconductor/normal/superconductor Josephson junctions microwave induced changes in the current-phase relation have been proposed<sup>15</sup> and observed,<sup>16</sup> based on a completely different mechanism; namely the microwave pumping produces a strong out-of-equilibrium quasiparticle distribution in the Andreev bound states in the normal metal.

## II. EXPERIMENT

We used superconductor/insulator/ferromagnet/superconductor (SIFS) Josephson junctions consisting of Nb(150 nm)/Al<sub>2</sub>O<sub>3</sub>/PdNi( $d_F$ )/Nb(50 nm) in a cross strip geometry [see Fig. 1(b)]. The ferromagnetic thin layer reduces the Josephson coupling and the phase relaxation time at the working temperature of 600 mK. The weak ferromagnet PdNi contains 10% of Ni, has a Curie temperature of around 150 K, and its thickness  $d_F$  varies between 50 and 100 Å.<sup>17</sup> We also fabricated nonferromagnetic (SIS) junctions without the PdNi layer, in order to verify that the thin ferromagnetic layer has no other effect than reducing the critical current.

The fabrication details are given elsewhere.<sup>17</sup> The critical current of ferromagnetic junctions is between 10 and 130  $\mu$ A, depending on  $d_F$ , the normal resistance  $R_n \sim 0.2 \Omega$ , and the critical temperature around 8.2 K. The junction area is  $0.7 \times 0.7 \text{ mm}^2$ , the capacitance  $C$  is 30 nF,<sup>14</sup> making phase dynamics underdamped.<sup>13</sup> The junction is directly connected to a 50- $\Omega$  coaxial cable by a superconducting stripe line. The electrical contact between the arm of the cable and the stripe line is ensured by silver epoxy. The attenuation in the rf line at 7 GHz is of about 30 dB. The magnetic field  $H$  is applied in the  $y$  direction. A  $\mu$ -metal shield ensures a negligible residual magnetic field in the one-shot <sup>3</sup>He cryostat.

In Fig. 1(a) we show the current-voltage ( $IV$ ) characteristic measured at zero applied magnetic field. The data follow a hysteretic  $IV$  characteristic with the retrapping current practically zero, as expected for strongly underdamped Josephson junctions. The plasma frequency  $\nu_p$  at zero applied magnetic field and zero bias current is 570 MHz. The resonance at  $V_1 = 15 \mu\text{V}$  (blue line) is the first Fiske step.<sup>18</sup> When a finite dc voltage appears across the junction, the cavity modes are resonantly excited at  $V_n^{\text{dc}} = \frac{h}{2e} \nu_n$ , and mix with the ac Josephson current giving rise to finite dc resonances.<sup>18</sup> The first Fiske step shown in Fig. 1(a) has been recorded separately for an applied magnetic field of  $\phi = 0.7\phi_0$  which maximizes the step amplitude. From  $V_1 = 15 \mu\text{V}$  we obtain a Swihart velocity  $\tilde{c} = 0.037c$ . In Fig. 1(a) we present only the first Fiske step but higher-order steps (not shown) are also observed.<sup>14</sup> We verify that the resonance at  $V_1 = 15 \mu\text{V}$  corresponds to the first Fiske resonance by measuring its magnetic field dependence  $I_{c1}(\phi)$ , as reported in Fig. 1(c) (blue line). For the current amplitude of the first Fiske step one obtains from theory<sup>19</sup>

$$I_{c1}(\phi) = b \cdot I_{c0} \left( \frac{4(\phi/\phi_0)}{2(\phi/\phi_0) + 1} \frac{\sin[\pi(\phi/\phi_0 - 0.5)]}{\pi(\phi/\phi_0 - 0.5)} \right)^2 \quad (4)$$

as experimentally observed. Equation (4) is plotted in Fig. 1(c) as a blue dashed line. Here the numerical constant  $b = 0.275$  is in the limit of high cavity quality factor  $Q_c$ . In Fig. 1(c) the critical current is also shown as a function of the applied magnetic field.  $I_c$  follows the Fraunhofer pattern (red dashed line) as described above. Smaller secondary maxima indicate a larger current density in the center of the junction.

We now focus on the effect of the intracavity field on the Josephson switching current, i.e., on the maximum superconducting current in the junction (at zero voltage bias), before it switches to the dissipative state, which corresponds to a finite voltage across the junction. In our junctions, at 600 mK, the switching current represents  $I_c$  within 1%.<sup>20</sup> The variation of the critical current as a function of the microwave frequency for a fixed microwave injected power of  $-15 \text{ dBm}$  is shown in Fig. 2(a). As a reference, we choose the microwave power provided by the source. The actual power at the sample is calibrated below. As microwaves are absorbed only at  $\nu = \nu_n$ , the critical current is suppressed only at resonance. This allows a fine spectroscopy of the cavity modes. We observed the first mode at 7.18 GHz as expected from the value measured for the first Fiske step (15  $\mu\text{V}$  correspond to 7.5 GHz). From the Lorentzian fit [see Fig. 2(a)], we obtain the cavity quality factor  $Q_c = 250$ .

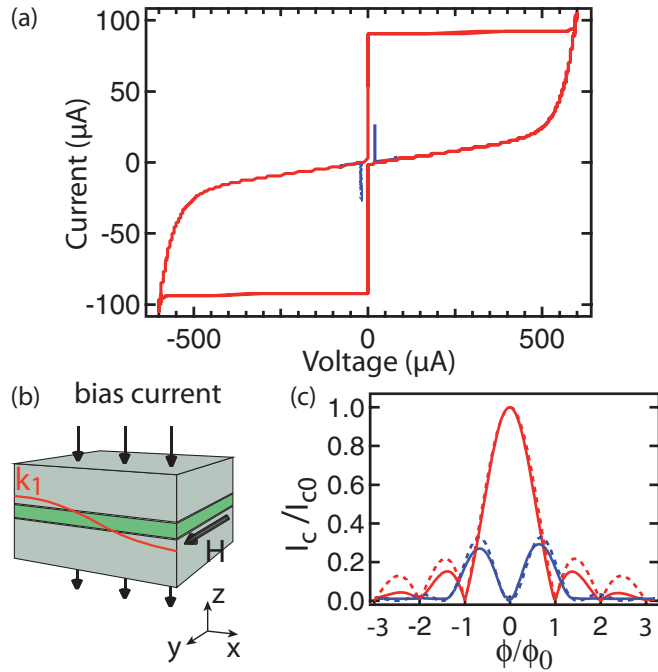


FIG. 1. (Color online) (a) Hysteretic current-voltage characteristic (red line) of extended Josephson junction, taken at 600 mK. The first Fiske resonance at  $V = 15 \mu\text{V}$  (blue line) is taken at  $\phi = 0.7\phi_0$ . (b) Sketch of extended Josephson junction. Electric-field distribution of the first resonant mode  $k_1$  is indicated in red. (c) Fraunhofer pattern of  $I_c$  (data: red line; theory: red dashed line), and first Fiske resonance  $I_{c1}$  (blue line) as a function of applied (in plane) magnetic field with theoretical curve (blue dashed line) given in the text by Eq. (4).

The quality factor is limited by dissipation. If dissipation is only due to quasiparticle tunneling,  $Q_c$  would be given by  $\omega_1 R_{qp} C$  (about  $4 \times 10^4$  in our junctions), where  $R_{qp}$  is the tunneling quasiparticle resistance. Nevertheless, it has been shown<sup>21</sup> that at high frequency, surface losses in the electrodes and dielectric losses in the insulator are more important than quasiparticle tunneling and they both substantially reduce  $Q_c$ .

The microwave induced suppression of the critical current at resonance is given by Eq. (3). At zero applied magnetic field the critical current reduces simply by  $\Delta I_c = I_c a_1^2/4$  as usually expected from photon-assisted Cooper pair tunneling.<sup>22</sup> We can use this formula to calibrate the actual rf power absorbed by the sample. In Fig. 2(b) we present  $I_c$  versus microwave power at resonance, i.e., for  $\nu = 7.18$  GHz. From the theoretical fit (blue line) we get the coupling constant,  $1 \times 10^{-4}$ , between the microwave circuit and the Josephson junction. This shows that the Josephson junction is weakly coupled to the microwave circuit.

We then sweep the magnetic field and for each value of the applied field, we measure the difference in the critical current  $\Delta I_c$  by subtracting  $I_c$  at two microwave frequencies 6.950 and 7.185 GHz for  $-15$  dBm microwave power, corresponding to  $-235$  and  $0$  MHz detuning from the first cavity mode, respectively. Note that 235 MHz is much larger than the cavity bandwidth.  $\Delta I_c$  as a function of the magnetic flux in the junction is reported in Fig. 2(c) (solid red line).  $\Delta I_c$  comes from the interference between the intracavity and the magnetic field, described by Eq. (3), which is also shown in

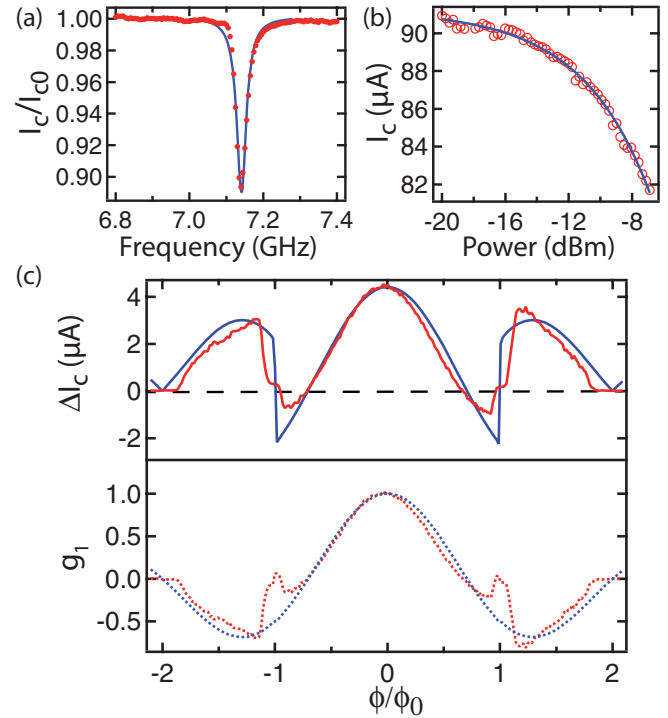


FIG. 2. (Color online) (a) Josephson spectroscopy of first cavity mode: Resonance of normalized critical current as function of microwave frequency (red dots) at  $\nu_1 = 7.18$  GHz with quality factor  $Q_c = 250$  from Lorentzian fit (blue line). (b) Suppression of critical current  $I_c$  as function of injected microwave power. Blue line corresponds to theoretical fit. (c) Deviation of the critical current  $\Delta I_c$  for resonant ( $\nu = 7.185$  GHz) and nonresonant ( $\nu = 6.950$  GHz) microwave excitation (red solid line). From this measurement the coupling constant  $g_1$  can be extracted experimentally (dotted red line) using Eq. (3). The blue solid line and blue dotted line are the theoretical predictions for  $\Delta I_c(\phi)$  and  $g_1(\phi)$  from Eqs. (3) and (1), respectively.

Fig. 2(c) (solid blue line). In particular, we observe the change in sign of  $\Delta I_c$  at  $0.7\phi_0$ . The jump at about  $\phi_0$  corresponds to the microwave induced  $\pi$ -0 transition in the macroscopic phase difference. Using Eq. (3) we extract  $g_1(\phi)$  from  $\Delta I_c(\phi)$ . The magnetic field dependence  $g_1(\phi)$  is reported in Fig. 2(c) (red dotted line) as well as the theoretical dependence of the coupling constant  $g_1(\phi)$  (blue dotted line) as expected from Eq. (1).

The change in sign of  $\Delta I_c$  can be seen more clearly in Fig. 3(a) where we plot the normalized critical current as a function of the microwave frequency and the applied magnetic field. The microwave power is  $-15$  dBm. Blue (red) corresponds to an increase (decrease) of the critical current. We observe that the frequency of the first resonance is slightly reduced by about 25 MHz, when  $\Delta I_c$  changes sign, i.e., for  $\phi > 0.7\phi_0$ . The resonance frequency at  $\phi = 0$  and  $\phi = 0.9\phi_0$  are marked by a dashed and a dotted line, respectively, in Fig. 3(a). This magnetic field induced shift in the resonance frequency  $\Delta\nu_1$  is smaller than, but comparable to, the cavity bandwidth and it explains the difference between data and theory in Fig. 2(c) for  $0.7 < (\phi/\phi_0) < 1$ . In fact, in this field range because of  $\Delta\nu_1$ , the value of  $\Delta I_c$  measured as the difference in the critical current at two microwave frequencies

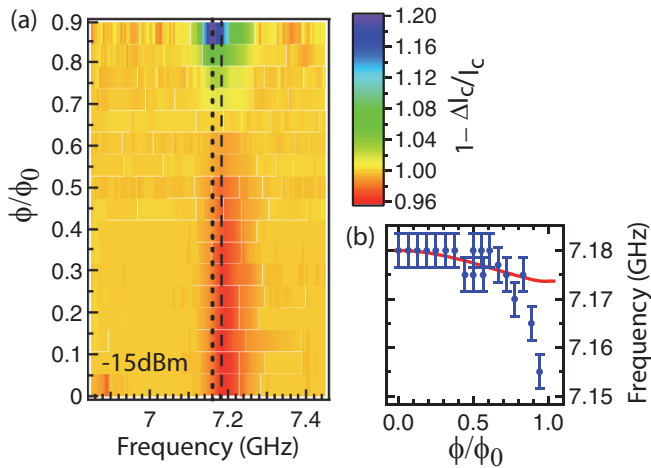


FIG. 3. (Color online) (a) Color map showing normalized deviation of critical current  $1 - \Delta I_c / I_c$  as a function of microwave frequency and applied magnetic field. (b) Variation of the microwave resonant frequency for applied magnetic field, deduced from (a). The red line corresponds to the theoretically expected variation of  $\nu_1$  as a function of an applied magnetic field.

6.950 and 7.185 GHz is underestimated, as can be seen in Fig. 2(c). In Fig. 3(b) we present the value of  $\Delta \nu_1$  obtained from the data in Fig. 1(a) as a function of the applied magnetic field. We verified that  $\Delta \nu_1$  is independent on the microwave power. Due to the Josephson coupling the dispersion of the electromagnetic waves in the junction is not linear; the cavity resonance frequencies become<sup>2</sup>  $\nu_n = \sqrt{\nu_p^2 + (k_n c_s)^2}$ , where  $\nu_p = 1/2\pi \sqrt{I_c / C \phi_0}$ . The red line accounts for  $\Delta \nu_1$  when the magnetic field dependence of the plasma frequency is

taken into account. As is clear from Fig. 3(b), the correction to  $\nu_1$  expected from the Josephson coupling is too small to explain the experimental changes observed in  $\nu_1$ . Therefore the shift in the resonance frequency  $\nu_1$  is likely related to the nonlinear dependence of the kinetic inductance of the electrodes on the magnetic field induced screening. This is of course a small correction but measurable because of the high quality factor of the cavity. Thus it is interesting to point out that the measurement of  $\nu_1$  is a very effective way to directly determine the kinetic inductance at finite frequency (GHz regime) of complex superconducting based multilayers.

### III. CONCLUSION

In conclusion, we have observed that the phase difference produced by an applied magnetic field together with the phase difference caused by the cavity intrafield due to microwave radiation interfere in extended Josephson junctions. This interference changes the Fraunhofer pattern of the critical current. The coupling strength between the intrafield and the Josephson phase is proportional to this interference term. By calibrating the actual rf power absorbed by the sample, we have directly measured this coupling. As it varies between  $-0.68$  and  $1$ , extended Josephson junctions provide an interesting device to address the ultrastrong coupling limit between the Josephson oscillator and the cavity eigenmodes.

### ACKNOWLEDGMENTS

We thank J. Gabelli, R. Gross, B. Reulet, and A. Ustinov and for valuable discussions. We are indebted to C. H. L. Quay for a critical reading of the manuscript.

\*apрили@lps.u-psud.fr

<sup>†</sup>Present address: Max-Planck-Institut für Quantenoptik, D-85748 Garching, Germany.

<sup>1</sup>A. Walraff, D. I. Schuster, A. Blais, L. Frunzio, R.-S. Huang, J. Majer, S. Kumar, S. M. Girvin, and R. J. Schoelkopf, *Nature (London)* **431**, 162 (2004).

<sup>2</sup>K. K. Likharev, *Rev. Mod. Phys.* **51**, 101 (1979).

<sup>3</sup>J. C. Swihart, *J. Appl. Phys.* **32**, 461 (1961).

<sup>4</sup>P. Nataf and C. Ciuti, *Phys. Rev. Lett.* **107**, 190402 (2011).

<sup>5</sup>M. V. Fistul and A. V. Ustinov, *Phys. Rev. B* **75**, 214506 (2007).

<sup>6</sup>In our junctions the ratio  $R = \nu_p / \nu_1$  is  $\sim 0.05$ , however, it is technically possible to achieve  $R \sim 1$ .

<sup>7</sup>S. Gröblacher, K. Hammerer, M. R. Vanner, and M. Aspelmayer, *Nature (London)* **460**, 724 (2009).

<sup>8</sup>F. Marquardt, J. P. Chen, A. A. Clerk, and S. M. Girvin, *Phys. Rev. Lett.* **99**, 093902 (2007).

<sup>9</sup>T. Niemczyk, F. Deppe, H. Huebl, E. P. Menzel, F. Hocke, M. J. Schwarz, J. J. Garcia-Ripoll, D. Zueco, T. Hümmer, E. Solano, A. Marx, and R. Gross, *Nat. Phys.* **6**, 772 (2010).

<sup>10</sup>H. Walther, B. T. H. Varcoe, B. G. Englert, and T. Becker, *Rep. Prog. Phys.* **69**, 1325 (2006).

<sup>11</sup>G. Gunter, A. A. Anappara, J. Hees, A. Sell, G. Biasiol, L. Sorba, S. De Liberato, C. Ciuti, A. Tredicucci, A. Leitensdorfer, and R. Huber, *Nature (London)* **458**, 178 (2009).

<sup>12</sup>R. C. Jaklevic, J. Lambe, J. E. Mercereau, and A. H. Silver, *Phys. Rev.* **140**, A1628 (1965).

<sup>13</sup>A. Barone and G. Paterno, *Physics and Applications of the Josephson Effect* (Wiley, New York, 1982).

<sup>14</sup>J. Hammer, M. Aprili, and I. Petkovic, *Phys. Rev. Lett.* **107**, 017001 (2011).

<sup>15</sup>Pauli Virtanen, T. T. Heikkilä, F. S. Bergeret, and J. C. Cuevas, *Phys. Rev. Lett.* **104**, 247003 (2010).

<sup>16</sup>M. Fuechsle, J. Bentner, D. A. Rynndyk, M. Reinwald, W. Wegscheider, and C. Strunk, *Phys. Rev. Lett.* **102**, 127001 (2009).

<sup>17</sup>T. Kontos, M. Aprili, J. Lesueur, F. Genet, B. Stephanidis, and R. Boursier, *Phys. Rev. Lett.* **89**, 137007 (2002).

<sup>18</sup>D. D. Coon and M. D. Fiske, *Phys. Rev.* **432**, A744 (1965).

<sup>19</sup>I. O. Kulik, *Sov. Phys. Tech. Phys.* **12**, 111 (1967).

<sup>20</sup>I. Petkovic and M. Aprili, *Phys. Rev. Lett.* **102**, 157003 (2009).

<sup>21</sup>R. F. Broom and P. Wolf, *Phys. Rev. B* **16**, 3100 (1977).

<sup>22</sup>S. Shapiro, *Phys. Rev. Lett.* **11**, 80 (1963).